



This is a repository copy of *Indium arsenide electron avalanche photodiodes for femtowatt level infrared detection*.

White Rose Research Online URL for this paper:

<https://eprints.whiterose.ac.uk/220695/>

Version: Accepted Version

---

### Proceedings Paper:

Blain, T. [orcid.org/0000-0002-7974-7355](https://orcid.org/0000-0002-7974-7355), Basta, G., Tan, C.H. [orcid.org/0000-0002-8900-9452](https://orcid.org/0000-0002-8900-9452) et al. (1 more author) (2024) Indium arsenide electron avalanche photodiodes for femtowatt level infrared detection. In: Berghmans, F. and Zergioti, I., (eds.) Optical Sensing and Detection VIII. SPIE Photonics Europe, 07-12 Apr 2024, Strasbourg, France. Proceedings of SPIE, 12999 . SPIE ISBN 9781510673168

<https://doi.org/10.1117/12.3022598>

---

© 2024 The Authors. Except as otherwise noted, this author-accepted version of a paper published in Proceedings of SPIE: Optical Sensing and Detection VIII is made available via the University of Sheffield Research Publications and Copyright Policy under the terms of the Creative Commons Attribution 4.0 International License (CC-BY 4.0), which permits unrestricted use, distribution and reproduction in any medium, provided the original work is properly cited. To view a copy of this licence, visit <http://creativecommons.org/licenses/by/4.0/>

### Reuse

This article is distributed under the terms of the Creative Commons Attribution (CC BY) licence. This licence allows you to distribute, remix, tweak, and build upon the work, even commercially, as long as you credit the authors for the original work. More information and the full terms of the licence here: <https://creativecommons.org/licenses/>

### Takedown

If you consider content in White Rose Research Online to be in breach of UK law, please notify us by emailing [eprints@whiterose.ac.uk](mailto:eprints@whiterose.ac.uk) including the URL of the record and the reason for the withdrawal request.



[eprints@whiterose.ac.uk](mailto:eprints@whiterose.ac.uk)  
<https://eprints.whiterose.ac.uk/>

# Indium Arsenide Electron Avalanche Photodiodes for Femtowatt Level Infrared Detection

T. Blain, G. Basta, C. H. Tan, J. S. Ng

Department of Electronic and Electrical Engineering, The University of Sheffield, S3 7 HQ, UK.

## ABSTRACT

Sensing of weak photon fluxes in the short to mid-wave infrared is important for a variety of applications such as optical communication systems, light detection and ranging (LiDAR) and remote gas sensing. For the most demanding applications, avalanche photodiodes (APDs) are regularly employed due to the enhanced sensitivity afforded by their internal avalanche gain. Indium Arsenide (InAs) is a material which exhibits near ideal avalanche multiplication properties and is capable of detecting infrared radiation up to 3  $\mu\text{m}$  at 77 K. Due to exclusive multiplication of electrons, it exhibits incredibly low excess noise factors below 2, regardless of the magnitude of avalanche gain. Furthermore, unlike most APD technologies, its bandwidth is not limited by its avalanche gain, allowing it to operate at high speeds with high gains. Using our recently developed planar process, we report InAs avalanche photodiodes which exhibit high gains in excess of 100 and external quantum efficiencies at 1550 nm of 56 %. Our liquid nitrogen cooled detectors are combined with a low noise current amplifier and the performance of the system is analyzed. Detection of weak 1550 nm laser pulses corresponding to <70 photons per pulse is demonstrated. The detector's noise current is shown to be background limited, hence, detection of lower optical powers could be achieved through further set-up optimization.

**Keywords:** Avalanche Photodiodes, InAs, excess noise, photodetector, SWIR, impact ionization.

## 1. INTRODUCTION

Avalanche photodiodes (APDs) are an excellent detector choice for applications which require detection of weak photon fluxes. Due to their internal gain mechanism, they are able to resolve signals which would otherwise be dominated by the noise components of downstream electronics (such as transimpedance amplifiers, comparators and analog-to-digital converters). The signal-to-noise ratio (SNR) enhancement of an avalanche photodiode operating with a transimpedance amplifier can be predicted using

$$SNR = \frac{RP_{sig}}{2qFI_d\Delta f + \frac{n_{amp}^2}{M^2}},$$

where  $R$  is the detectors responsivity,  $P_{sig}$  is the signal optical power,  $q$  is the elementary charge,  $F$  is the APDs excess-noise factor,  $\Delta f$  is the bandwidth of the measurement,  $n_{amp}$  is the amplifiers input referred noise current and  $M$  is the APDs avalanche gain. Compared to a conventional photodiode, the contribution to the total noise level from the amplifier is effectively reduced by a factor of  $M^2$ . However, it is also clear from the SNR equation that the APDs dark current and excess noise factor must also be kept low to provide the maximum SNR enhancement. The excess noise factor of an APD is a result of the stochastic nature of the avalanche multiplication process. From multiplication theory proposed by McIntyre[1], the excess noise factor of an APD can be related to the ionization coefficients of electrons and holes using

$$F = kM + (1 - k) \left( 2 - \frac{1}{M} \right),$$

where  $k$  is the ratio of the electron and hole ionization coefficients. It is clear from the equation for  $F$  that avalanching materials with highly disparate ionization coefficients provide the lowest excess noise. In the ideal case where one of the ionization coefficients is zero (and hence  $k = 0$ ),  $F$  asymptotically approaches 2 with increasing  $M$ . Hence, there is very little excess noise penalty for operating the APD with high avalanche gain. There are two main approaches to producing APDs with  $k = 0$ . One is to use impact ionization engineered structures which suppress the ionization rate of one carrier type. These include staircase structures which were proposed by Capasso [2] and were recently demonstrated to provide deterministic gain with low excess noise [3]. This approach however is complex and high avalanche gains are yet to be demonstrated. A much simpler approach is to utilize materials which intrinsically exhibit  $k = 0$  due to their band structures.

Such materials include: HgCdTe, InSb and InAs. Due to the exclusive multiplication of electrons in APDs constructed from these materials, they are part of a class of APDs termed electron-APDs (eAPDs). HgCdTe eAPDs have been demonstrated to exhibit high gains in excess of 600 with  $F \sim 1$ . These structures are however complex to grow, toxic and require costly CdZnTe substrates [4]. InSb eAPDs suffer greatly from high band-to-band tunneling currents due to its very narrow bandgap (0.17 eV) hence, only limited avalanche gains have been demonstrated ( $\sim 3$ ) [5]. Gains in excess of 100 have been demonstrated using InAs eAPDs with  $F \sim 1.6$ . These detectors have potential to be useful in SWIR applications up to a detection wavelength of 3  $\mu\text{m}$  such as Light-Detection-And-Ranging (LiDAR) and Differential-Absorption-LiDAR (DiAL) for monitoring of common atmospheric gasses such as  $\text{CHF}_3$  [6] and  $\text{CO}_2$  [7]. Here we demonstrate the low-photon-level detection capabilities of recently developed planar InAs eAPDs.

## 2. GROWTH, FABRICATION AND EXPERIMENTAL DETAILS

InAs epilayers were grown on 100 orientated 2" InAs substrates. The device structure consisted of a 600 nm  $n$ -type InAs layer doped with Si followed by a thick 9.6  $\mu\text{m}$  intrinsic InAs layer. The  $p$ -type region was formed using Be ion implantation. The wafer was patterned with resist and subjected to a Be implant cycle with an energy of 45 keV and dose of  $2.3 \times 10^{14} \text{ cm}^{-2}$  to produce a shallow  $\sim 200 \text{ nm}$   $p$ -type region. The detectors were metalized with Ti/Au top and bottom contacts and passivated with SU8. Finally, Ti/Au bondpads were deposited after deposition of a 200 nm SiN layer to provide electrical isolation between the bondpads and the InAs surface. A scanning electron microscope image of a fully fabricated  $200 \times 200 \mu\text{m}^2$  pixel is shown in fig. 1.

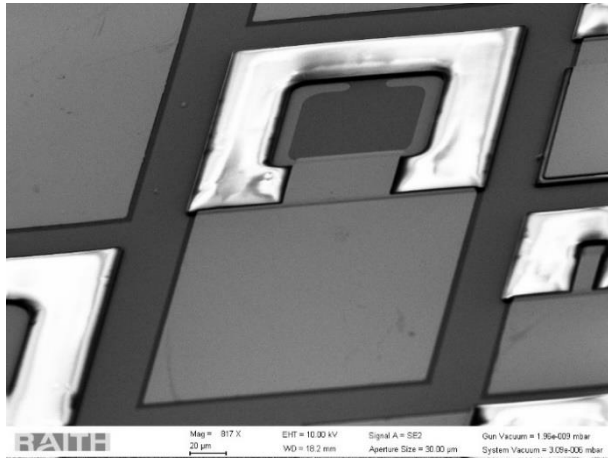


Fig. 1. Scanning electron microscope image of a  $200 \times 200 \mu\text{m}^2$  InAs eAPD.

The devices were ball-wire bonded onto TO-5 headers and cooled in a liquid nitrogen dewar to  $\sim 140 \text{ K}$  to be characterized. The optical signal was coupled to the detectors inside the dewar via a kBr window. Optical measurements were performed using a 10 kHz modulated 1.55  $\mu\text{m}$  diode laser and the optical power was controlled using a variable attenuator. The bias of the devices was controlled using a source-measure-unit. The output current from the detectors was amplified using a transimpedance amplifier with a gain of  $10^5 \text{ V/A}$ , a bandwidth of 200 kHz and an input referred current noise density of  $\sim 1 \text{ pA/Hz}^{-1/2}$ . The output of the amplifier was measured using an FFT spectrum analyzer. A diagram of experimental setup is presented in fig. 2.

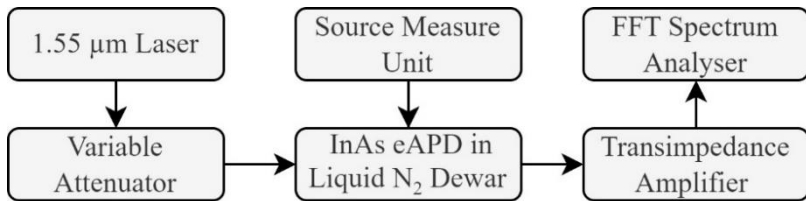


Fig. 2. Experimental set-up for InAs eAPD characterization.

### 3. RESULTS & DISCUSSION

These devices were found to exhibit higher 1.55  $\mu\text{m}$  responsivities than previous reports of planar InAs eAPDs at 0.7 A/W corresponding to a 56 % external quantum efficiency (EQE). A comparison between previously reported Be implant conditions and responsivities for planar InAs eAPDs is shown in table 1.

Table 1. Comparison of implantation conditions and 1.55  $\mu\text{m}$  responsivity of planar InAs eAPDs

Ref.	Implant Energy (keV)	Implant Dose ( $\text{cm}^{-2}$ )	Projected Range (nm)	Responsivity (A/W)	EQE (%)
[8]	190 + 70	$1 \times 10^{14} + 2.8 \times 10^{13}$	645	0.46	37
[9]	34	$2 \times 10^{14}$	100	0.62	51
This Work	45	$2.3 \times 10^{14}$	200	0.7	54

We believe that the higher EQE compared to the devices from [8] is due to the shallower implant depth used, resulting in a higher portion of carriers being absorbed close to/inside of the devices' depletion region. Compared to the devices in [9], we believe the higher EQE can be attributed to the wafer quality, since the devices from [9] were shown to have generation-recombination limited dark current at room temperature while the ones presented here exhibited diffusion limited dark current down to  $\sim 180$  K.

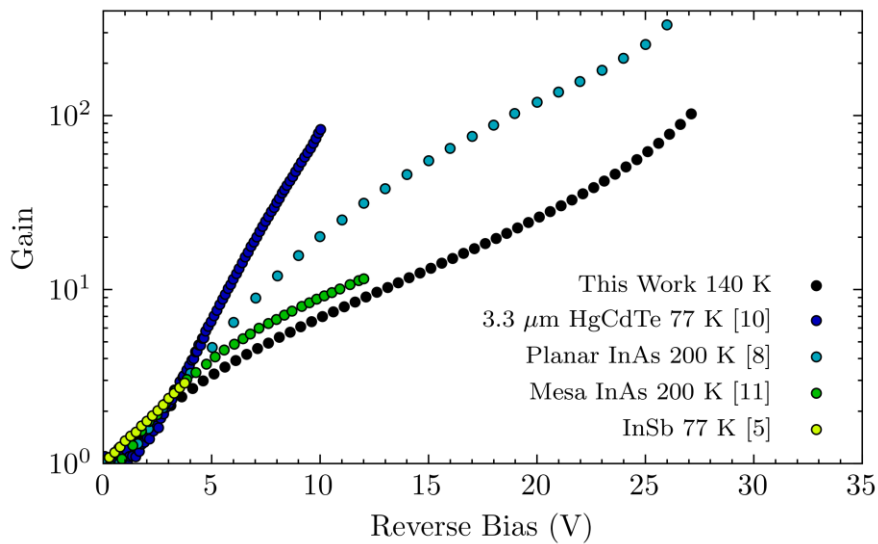


Fig. 3. Measured 1550 nm avalanche gain (at an operating temperature of  $\sim 140$  K) compared with a 3.3  $\mu\text{m}$  cut-off HgCdTe eAPD [10], a InSb eAPD [5] as well as previously reported mesa [11] and planar [8] InAs eAPDs operating at 200 K.

The avalanche gain of the detectors measured at 140 K is presented in fig. 3 and compared HgCdTe (using a composition with a similar cut-off to InAs) and InSb both operating at 77 K as well as previously reported planar and mesa InAs eAPDs operating at 200 K. A maximum gain of 104 was achieved at 27.5 V. The lower gain compared with the InAs detectors from [8] is partially due to the lower temperature used here (since InAs exhibits a positive temperature dependence of electron ionization) as well as the fact that the depletion width is thinner in the eAPDs presented here.

The gain, responsivity, dark current and gain normalized dark current are shown in fig. 4 for an  $80 \times 80 \mu\text{m}$  pixel operating at 140 K. The reverse current of the detectors was found to be background limited due to insufficient shielding. This was verified by comparing the IVs measured in a separate temperature controlled helium cryostat at different temperatures using a solid metal cap on the TO-5 headers to block the black-body radiation. This data is shown in fig. 5. We find that there is little benefit in cooling the detectors much below  $\sim 180$  K in terms of current reduction. Further optimizations of the packaging/cooling of the detectors, such as including a cooled band-pass optical filter, are required to reduce the background limited current at lower temperatures.

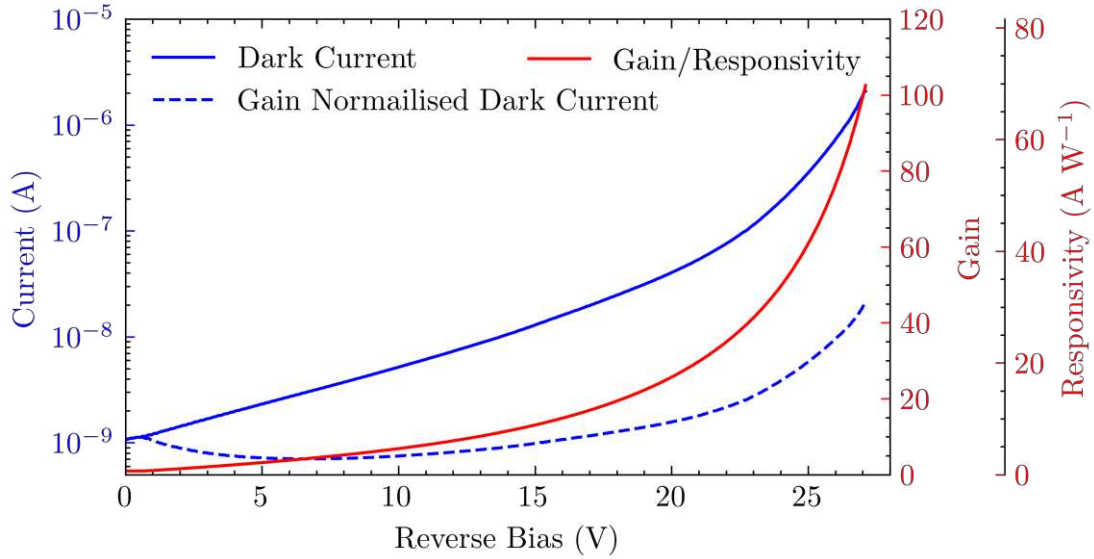


Fig. 4. 1550 nm responsivity, gain, dark current and gain normalized dark current of an  $80 \times 80 \mu\text{m}$  pixel operating at  $\sim 140 \text{ K}$ .

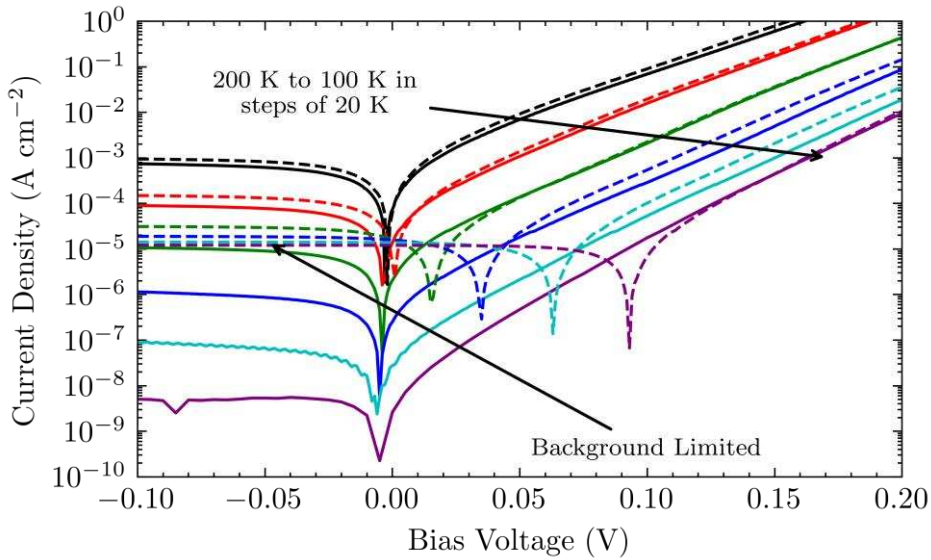


Fig. 5. Comparison of the temperature dependence of the current-voltage characteristics between detectors with (dashed lines) and without (solid lines) cooled metal caps fitted to the TO-5 headers.

The output FFT spectra, measured under different bias voltages with the detectors illuminated with a 1550 nm 10 kHz modulated laser are shown in fig. 6 with an average power of 8.77 pW. The noise floor of the measurement was observed to increase for reverse bias voltages  $> 22.5 \text{ V}$ . This increase was attributed to the dominance of band-to-band tunneling currents at these bias voltages. The SNR was calculated from the magnitude of the signal peaks and the mean noise level in the adjacent frequency bins. The maximum SNR occurred around a gain of 54. The detectors were biased to this gain and the optical power was attenuated further. The normalized FFT spectra under low optical power levels are presented in fig. 8. For average optical powers as low as 88 fW, the signal peak was still clearly discernable from the noise floor, corresponding to  $\sim 70$  photons per  $50 \mu\text{s}$  pulse.

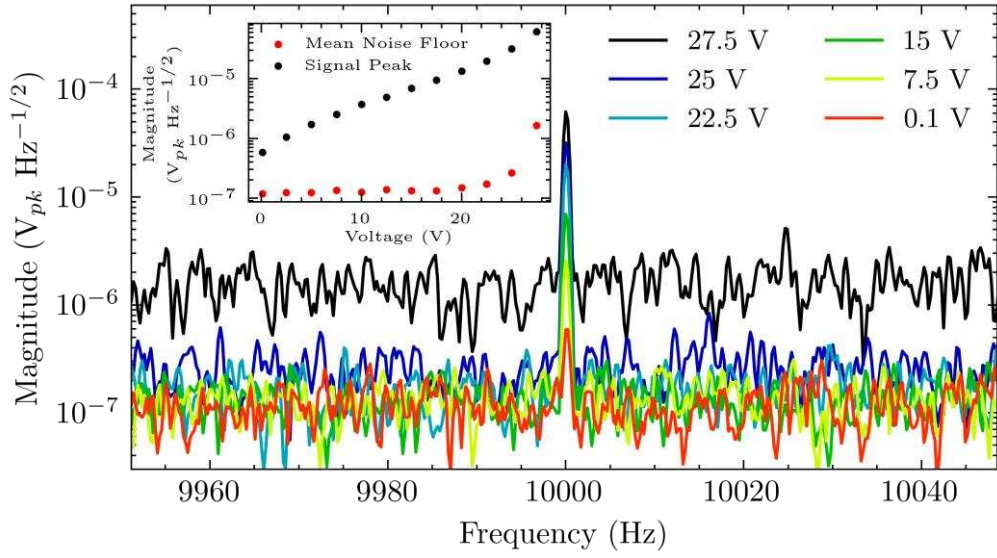


Fig. 6. Output FFT spectra from the transimpedance amplifier with the detector biased at different reverse bias voltages. The inset plot shows the bias dependence of the signal peaks and noise floor.

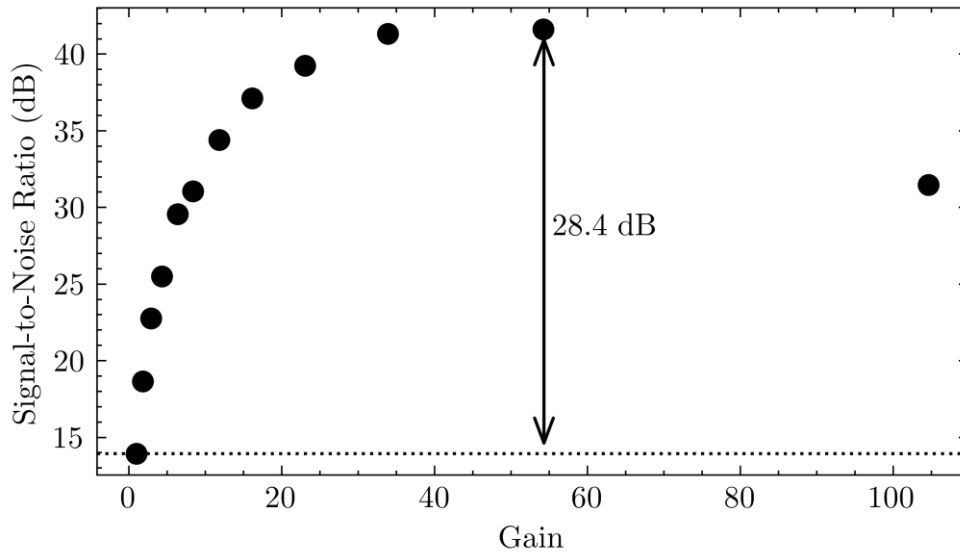


Fig. 7. SNR calculated from the data in fig. 6.

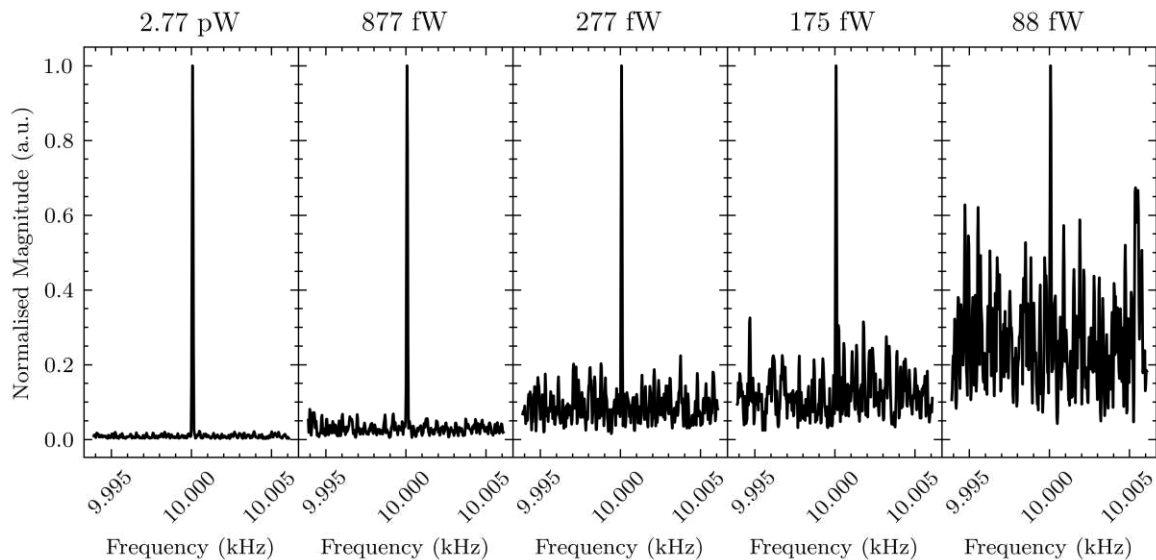


Fig. 8. Output FFT spectra for decreasing optical powers with the detector reverse bias voltage held at 22.5 V

#### 4. CONCLUSIONS

Planar InAs eAPDs have been produced with high 1550 nm responsivity (0.7 A/W) and gain (exceeding 100). Combining with a transimpedance amplifier, detection of weak optical signals corresponding to <70 photons per 50  $\mu$ s pulse. It was established that the dark current of these detectors is currently limited by background radiation. Elimination of this component could lead to >1 order of magnitude lower reverse current at 140 K and >4 orders of magnitude lower at 100 K. Hence, the performance of these InAs eAPDs could be further enhanced through set-up level optimizations such as the inclusion of cooled optical filters.

#### ACKNOWLEDGEMENTS

This work was funded by the Engineering and Physical Sciences Research Council (EPSRC) reference no: EP/S026428/1.

#### REFERENCES

- [1] R. J. McIntyre, 'Multiplication noise in uniform avalanche diodes', *IEEE Transactions on Electron Devices*, vol. ED-13, no. 1, pp. 164–168, Jan. 1966, doi: 10.1109/T-ED.1966.15651.
- [2] F. Capasso, Won-Tien Tsang, and G. F. Williams, 'Staircase solid-state photomultipliers and avalanche photodiodes with enhanced ionization rates ratio', *IEEE Trans. Electron Devices*, vol. 30, no. 4, pp. 381–390, Apr. 1983, doi: 10.1109/T-ED.1983.21132.
- [3] A. A. Dadey, A. H. Jones, S. D. March, S. R. Bank, and J. C. Campbell, 'Near-unity excess noise factor of staircase avalanche photodiodes', *Optica*, vol. 10, no. 10, p. 1353, Oct. 2023, doi: 10.1364/OPTICA.496587.
- [4] W. Lei, J. Antoszewski, and L. Faraone, 'Progress, challenges, and opportunities for HgCdTe infrared materials and detectors', *Applied Physics Reviews*, vol. 2, no. 4, p. 041303, Dec. 2015, doi: 10.1063/1.4936577.
- [5] J. Abautret, J. P. Perez, A. Evirgen, J. Rothman, A. Cordat, and P. Christol, 'Characterization of midwave infrared InSb avalanche photodiode', *Journal of Applied Physics*, vol. 117, no. 24, p. 244502, Jun. 2015, doi: 10.1063/1.4922977.
- [6] F. Innocenti, R. Robinson, T. Gardiner, A. Finlayson, and A. Connor, 'Differential Absorption Lidar (DIAL) Measurements of Landfill Methane Emissions', *Remote Sensing*, vol. 9, no. 9, p. 953, Sep. 2017, doi: 10.3390/rs9090953.
- [7] U. N. Singh, T. F. Refaat, M. Petros, and S. Ismail, 'Evaluation of 2-  $\mu$  m Pulsed Integrated Path Differential Absorption Lidar for Carbon Dioxide Measurement—Technology Developments, Measurements, and Path to

- Space', *IEEE J. Sel. Top. Appl. Earth Observations Remote Sensing*, vol. 11, no. 6, pp. 2059–2067, Jun. 2018, doi: 10.1109/JSTARS.2017.2777453.
- [8] B. S. White *et al.*, 'High-Gain InAs Planar Avalanche Photodiodes', *Journal of Lightwave Technology*, vol. 34, no. 11, pp. 2639–2644, Jun. 2016, doi: 10.1109/JLT.2016.2531278.
- [9] L. W. Lim, C. H. Tan, J. S. Ng, J. D. Petticrew, and A. B. Krysa, 'Improved Planar InAs Avalanche Photodiodes With Reduced Dark Current and Increased Responsivity', *J. Lightwave Technol.*, vol. 37, no. 10, pp. 2375–2379, May 2019, doi: 10.1109/JLT.2019.2905535.
- [10] J. Rothman *et al.*, 'High operating temperature SWIR HgCdTe APDs for remote sensing', presented at the SPIE Security + Defence, M. T. Gruneisen, M. Dusek, J. G. Rarity, K. L. Lewis, R. C. Hollins, T. J. Merlet, and A. Toet, Eds., Amsterdam, Netherlands, Oct. 2014, p. 92540P. doi: 10.1117/12.2069486.
- [11] I. C. Sandall, S. Zhang, and C. H. Tan, 'Linear array of InAs APDs operating at 2  $\mu\text{m}$ ', *Opt. Express*, vol. 21, no. 22, p. 25780, Nov. 2013, doi: 10.1364/OE.21.025780.